JACS
JOURNAL OF THE AMERICAN CHEMICAL SOCIETY

COMMUNICATION

pubs.acs.org/JACS

High-Resolution 2D *J*-Resolved Spectroscopy in Inhomogeneous Fields with Two Scans

Yulan Lin, Zhiyong Zhang, Shuhui Cai, and Zhong Chen*

Department of Electronic Science and Fujian Key Laboratory of Plasma and Magnetic Resonance, State Key Laboratory of Physical Chemistry of Solid Surfaces, Xiamen University, Xiamen, Fujian 361005, China

Supporting Information

ABSTRACT: A scheme via spatially encoded intermolecular zero-quantum coherences was proposed for high-resolution 2D *J*-resolved spectra in inhomogeneous fields with high acquisition efficiency. Compared to a recent paper (Pelupessy et al. *Science*, **2009**, *324*, 1693−1697), the novel method can obtain chemical shifts and *J* multiplicity patterns directly.

Nuclear magnetic resonance spectroscopy has been used to study organic chemistry, dynamic effect, protein and nucleic acid structure, and function. It delivers detailed molecular-level information, such as chemical shifts and *J*-couplings, revealing subtle differences in the environments of various nuclei. This in turn demands a highly homogeneous magnetic field B_0, with spatial variations below about 10^{-9}. However, it is often not possible to work under ideal conditions. For example, achieving such homogeneity is not trivial when dealing with samples subject to substantial internal susceptibility distortions,[1] when employing remote NMR arrangements,[2] and when using resistive or hybrid magnets.[3]

Many techniques have been proposed to collect high-resolution NMR spectra in the presence of field distortions. One of the earliest and still most widely used methods is spin-echo, which can refocus the phases accumulated by inhomogeneous B_0 field and demonstrate *J*-couplings, but completely eliminate chemical shifts.[4] In recent years, some approaches to compensate the field inhomogeneity have been proposed by the use of custom-built radio frequency (RF) coils. They employ either an inhomogeneous RF field to match the inhomogeneous B_0 field[5] or field gradients along with RF pulses to compensate the phase accumulation due to the inhomogeneous B_0 field in one dimension.[6] They all need a prior description of the spatial dependence of the B_0 magnetic field. Khaneja and co-workers proposed a Fourier synthesis algorithm to design phase-compensating RF pulses and pulsed-field gradients to obtain high-resolution spectra in arbitrarily spatially dependent inhomogeneous fields.[7] In addition, several methods based on intermolecular multiple-quantum coherences (iMQCs) were also proposed to obtain high-resolution NMR spectra in inhomogeneous and unstable fields.[8] However, since 2D or 3D acquisition is necessary for a high-resolution 1D or 2D spectrum, the long acquisition time limits their applications. More recently, a *J*-coupling coherence transfer scheme was combined with a spatially encoded technique[9] to achieve high-resolution *J*-resolved-like spectra in fields with large inhomogeneity.[10] This method takes advantage of fast acquisition (in the order of milliseconds). However, it is the differences of the precession frequencies of any two scalar-coupled spins and *J*-couplings information that are shown in the F1 and F2 dimensions, respectively, which makes direct spectral assignments challenging. Moreover, uncoupled spins (singlets) cannot be detected by this method. In addition, the middle peak of any multiplet with odd splitting is missed (i.e., the peak amplitude is zero). In the present study, we propose another coherence transfer scheme to achieve narrow lines in the presence of B_0 heterogeneities, which combines intermolecular zero-quantum coherence (iZQC) with spatial encoding and does not suffer from the aforementioned problems.

Without loss of generality, we consider a homogeneous liquid mixture consisting of *S* and *I* components. *S* is an *AX* spin-$^1/_2$ system taken as solute (including S_k and S_l spins with a scalar coupling constant J_{kl}), and *I* is a single spin-$^1/_2$ system taken as solvent. In Figure 1A, the *J*-coupling coherence transfer scheme combined with spatial encoding proposed by Pelupessy et al.[10] is shown. During the first spatially encoded block (comprising a linearly swept adiabatic 180° pulse and a gradient G_E), the coherence S_k^- is spatially encoded. At the end of this block, S_k^- is transferred to $S_k^+ S_{lz}$ with a phase

$$\varphi_{S_k}(z) = -[\omega_{S_k} + \gamma\delta B_0(z) + \gamma G_E z]^2/R - O_i^2/R \qquad (1)$$

where ω_{S_k} is the chemical shift of the S_k spin, γ is the gyromagnetic ratio, and $\delta B_0(z)$is the unknown inhomogeneous magnetic field.[10] For simplicity, $\delta B_0(z)$ is assumed to be along the *z* axis. O_i is the initial frequency offset of the adiabatic 180° RF pulse, and the sweep rate $R = \Delta\omega_{ad}/\tau_{ad}$, given by the ratio between the sweep width $\Delta\omega_{ad}$ and the duration τ_{ad} of the adiabatic pulse. After the second 90° RF pulse, the coherence $S_k^+ S_{l_z}$ is transferred to $S_{k_z} S_l^+$ though *J*-coupling. After the second spatially encoded block, which is the same as the first one, the coherence $S_{k_z} S_l^+$ is transferred to $S_{k_z} S_l^-$ with a phase

$$\varphi_{S_l}(z) = [\omega_{S_l} + \gamma\delta B_0(z) + \gamma G_E z]^2/R + O_i^2/R \qquad (2)$$

where ω_{S_l} is the chemical shift of the S_l spin. Before acquisition, the total phase of the coherence $S_{k_z} S_l^-$ is the sum of the phases accumulated by each term:

$$\varphi_S(z) = \varphi_{S_k}(z) + \varphi_{S_l}(z) = (\omega_{S_l}^2 - \omega_{S_k}^2)/R + 2\gamma(\omega_{S_l} - \omega_{S_k})(\delta B_0(z) + G_E z)/R \qquad (3)$$

Received: December 16, 2010
Published: April 27, 2011

dx.doi.org/10.1021/ja1113479 | *J. Am. Chem. Soc.* 2011, 133, 7632–7635

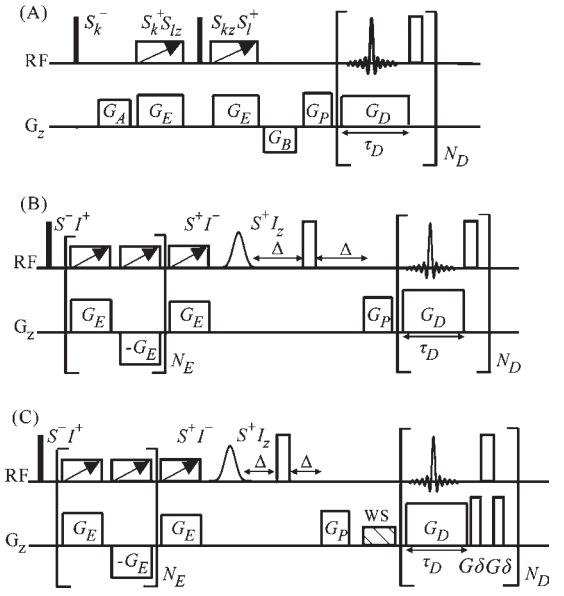

Figure 1. Pulse sequences for high-resolution NMR spectra in arbitrarily inhomogeneous fields. (A) *J*-coupling coherence transfer scheme combined with spatial encoding proposed by Pelupessy et al.[10] (B) Intermolecular zero-quantum coherence transfer scheme combined with spatial encoding proposed in this work. Multi-echo excitation is incorporated to limit the effects of molecular diffusion. (C) Incorporating water suppression block into scheme B to suppress the solvent signal. Solid and open vertical rectangles represent 90° and 180° RF pulses. The rectangles with sloping arrows indicate adiabatic frequency-swept 180° pulses. The Gauss-shaped pulse is the 90° solvent-selective RF pulse. G_E and G_D are encoding and decoding gradients. The gradients G_A and G_B of equal area serve to select the desired coherence transfer pathway. The gradient G_P prior to acquisition is adjusted to set the middle of the chemical shift range in the middle of the detection period τ_D. "WS" represents the solvent suppression module. The gradients of area $G\delta$ serve to remove the residual solvent signal.

When a decoding gradient G_D with the same amplitude as the encoded gradient G_E is applied, an echo will appear at $t_D = 2(\omega_{S_k} - \omega_{S_l})/R$. Since the *J*-modulated detection scheme[11] is added as a second dimension, the signals in the resulting 2D spectrum will then located at $(\omega_{S_k} - \omega_{S_l}, \pm\pi J_{kl})$ and $(\omega_{S_l} - \omega_{S_k}, \pm\pi J_{kl})$. This indicates that it is the chemical shift difference between the two *J*-coupled spins that is displayed in the F1 dimension, and the F2 dimension shows the *J*-coupling. Both dimensions are independent of $\delta B_0(z)$.

Figure 1B shows the pulse sequence we proposed. A multi-echo excitation[12] is incorporated to reduce the effect of molecular diffusion. A bipolar gradient pair with adiabatic pulses repeated N_E times is inserted before the adiabatic pulse. In this case, the amplitude of the decoding gradient should be $(2N_E + 1)$ times the amplitude of the encoding gradient to cancel the effect of inhomogeneous field $\delta B_0(z)$. For simplicity, we consider the case of $N_E = 0$ in our theoretical analysis. A 90° RF pulse excites the iZQC (S^-I^+ with coherence order $p = 0$, S represents either S_k or S_l). During the iZQC evolution period, a spatially encoded block is applied. The coherence S^-I^+ is transferred to S^+I^- with a phase

$$\varphi_{SI}(z) = \{[(\omega_I + \gamma\delta B_0(z) + \gamma G_E z)^2 + O_i^2] - [(\omega_S + \gamma\delta B_0(z) + \gamma G_E z)^2 + O_i^2]\}/R \quad (4)$$

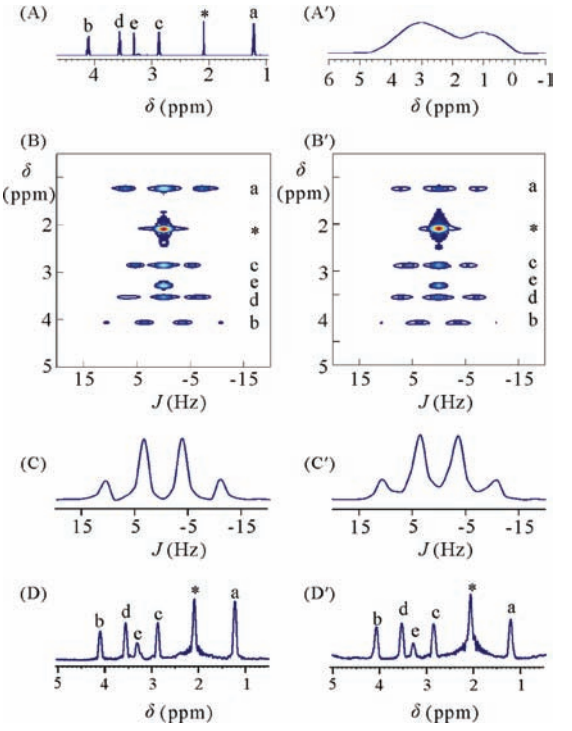

Figure 2. (A) Conventional 1D ^{1}H NMR spectrum of the solution of ethyl 3-bromopropionate ($BrCH_2^dCH_2^cCOOCH_2^bCH_3^a$) and methanol ($CH_3^eOH$) in acetone ($CH_3COCH_3$) (molar ratio 4:2:1) recorded in a homogeneous field. The peaks mared by * are solvent. (A′) Same, but in the presence of ~3.6 ppm (or 1.8 kHz at 500 MHz) field inhomogeneity artificially introduced by detuning the spectrometer's $\{z_1,x_1,y_1\}$ shim coils. (B,B′) 2D iZQC *J*-resolved spectra using the pulse sequence shown in Figure 1B, obtained in the homogeneous and inhomogeneous B_0 fields, respectively, as evident in the conventional 1D spectra in (A) and (A′). (C,C′) Projection along the F2 dimension of the quadruplet at 4.16 ppm in (B) and (B′) spectra, respectively. (D,D′) Accumulated projection along the F1 dimension (chemical shift axis) from (B) and (B′) spectra, respectively. The spectra are presented in magnitude mode. Both spectra were recoded with $N_E = 1$, $G_E = 0.7$ G/cm, and $G_D = 2.1$ G/cm. For homogeneous field, the WURST adiabatic pulse with 20 kHz sweep range was applied during 30 ms. For inhomogeneous field, the sweep range was 16 kHz, applied during 24 ms. $N_D = 80$ ($t_2^{max} = 560$ ms).

i.e.,

$$\varphi_{SI}(z) = (\omega_I^2 - \omega_S^2)/R + 2\gamma(\omega_I - \omega_S)(\delta B_0(z) + G_E z)/R \quad (5)$$

Comparing eq 5 with eq 3, we can see that φ_{SI} has the same form as φ_S.

After the 90° solvent-selective RF pulse, the coherence S^+I^- is transferred to S^+I_z through the action of distant dipolar field (DDF). With the same detection scheme as Figure 1A, the signals in the resulting 2D spectrum will locate at $(\omega_S - \omega_I, \pm\pi J_{kl})$. So besides the *J*-coupling information shown in the F2 dimension, it is the chemical shift difference between the spins S and I instead of between two *J*-coupled spins that is shown in the F1 dimension. As all the peaks have a frequency shift of ω_I in the F1 dimension, we can set the spectrometer reference frequency to coincide with the frequency offset of I spin, i.e., $\omega_I = 0$, and then the signal location becomes $(\omega_S, \pm\pi J_{kl})$. Hence, the chemical shift as well as *J*-coupling information can be

dx.doi.org/10.1021/ja1113479 |*J. Am. Chem. Soc.* 2011, 133, 7632–7635

directly obtained from the resulting 2D spectrum. To prevent the dephasing of signals caused by the inhomogeneous magnetic field before the DDFs take effect, a 180° RF pulse is inserted in the middle of delay interval 2Δ (Figure 1B). (See Supporting Information for a detailed derivation for the signals from the pulse sequence shown in Figure 1B.)

Because of the use of selective pulse, in principle, the upper limit of field inhomogeneity resolvable by the sequence depends on the minimum difference in chemical shifts between the solvent and solute peaks. The method still works in the case of moderate inhomogeneous fields when the solvent peak partly overlaps the nearest solute resonances, as long as the effect of DDF produced by solvent due to partial excitation is strong enough to be detected.

In Figure 1C, the W5 binomial 180° RF pulse was used as a solvent-exclusive 180° pulse in the WS module to efficiently suppress solvent signal.[13] As T_1 relaxation will induce spurious solvent echo, giving rise to undesirable signals, we introduce two identical gradients, $G\delta$, on both sides of the 180° hard pulse in the detection period to eliminate this effect.

Figure 2 illustrates the potential of our method to retrieve high-resolution ^{1}H NMR data. The experiment was performed at 298 K using a Varian NMR System 500 MHz spectrometer (Varian, Palo Alto, CA), equipped with a 5 mm $^1H\{^{15}N-^{31}P\}$ indirect detection probe. The sample was a mixture of ethyl 3-bromopropionate, methanol, and acetone with a molar ratio of 4:2:1.The pulse sequence in Figure 1B was used with a two-step phase cycling: the phases for the Gauss-selective RF pulse and the receiver were $(x, -x)$. The phases of the 180° pulses during the decoding period were alternated between y and $-y$ every two increments. The length of the 90° Gauss-shaped RF pulse was 12.75 ms, which corresponded to an excitation range of about 240 Hz. To produce an inhomogeneous field, the shim coils were intentionally deshimmed to produce a line width of about 1800 Hz. In the homogeneous and inhomogeneous fields, the frequency offset and the length of the Gauss-shaped pulse were kept unchanged, and the spectra were obtained with the same acquisition conditions and processed with the same parameters. As we can see, all multiplet structures (three triplets located at a, c, and d and one quadruplet located at b) are clearly visible in the 2D spectra. The isolated spins (CH_3 of methanol located at e) are also detected. The whole spectral pattern is the same as the conventional J-resolved spectrum. The solvent peak is located at 2.09 ppm. It mainly comes from the residual longitudinal magnetization due to longitudinal relaxation during the τ_{ad} period, which becomes detectable after the solvent-selective 90° RF pulse.[14] The average line widths of the solute peaks, measured from the projection spectra along the chemical shift axis (F1 dimension), are approximately 31.6 and 33.2 Hz (Figure 2D and D′, respectively). The resolution in the F1 dimension can be further improved by reducing the sweep rate R of the adiabatic pulse. In our experiments, we set R = 66.7 kHz/s, which seems to provide the best compromise between sensitivity and resolution. The resolution in the F1 dimension is also affected by the residual field inhomogeneity within the dipolar correlation distance, which is more severe in large inhomogeneous fields than in homogeneous fields. The resolution in the F2 dimension is satisfactory compared to the conventional 2D high-resolution J-resolved spectrum and should be sufficient for most J-resolved experiments. The signal-to-noise ratios (SNRs) in Figure 2D,D′ are 292 and 125, respectively. The lower SNR in Figure 2D′ is mainly due to the faster signal attenuation in the inhomogeneous field. The SNR was measured

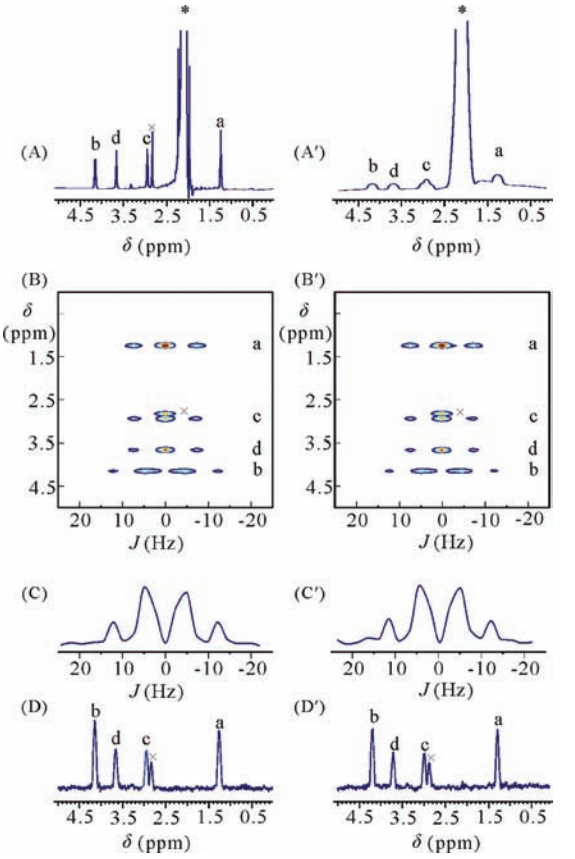

Figure 3. (A) Conventional 1D ^{1}H NMR spectrum of the solution of 97 mM ethyl 3-bromopropionate ($BrCH_2^dCH_2^cCOOCH_2^bCH_3^a$) in acetone ($CH_3COCH_3$) recorded in a homogeneous field. The peaks marked by * are solvent. The peak (marked by ×) at 2.83 ppm is from the protons of residual water in the sample. (A′) Same, but in the presence of ~0.22 ppm (or 110 Hz at 500 MHz) field inhomogeneity artificially introduced by detuning the spectrometer's $\{z_1,x_1,y_1\}$ shim coils. (B,B′) 2D iZQC J-resolved spectra using the pulse sequence shown in Figure 1C, obtained in the homogeneous and inhomogeneous B_0 fields, respectively, as evident in the conventional 1D spectra in (A) and (A′). (C,C′) Projection along the F2 dimension of the quadruplet at 4.16 ppm in (B) and (B′) spectra, respectively. (D,D′) Accumulated projection along the F1 dimension (chemical shift axis) from (B) and (B′) spectra, respectively. The spectra are presented in magnitude mode. Both spectra were recoded with N_E = 1, G_E = 0.7 G/cm, and G_D = 2.1 G/cm. The WURST adiabatic pulse with 20 kHz sweep range was applied during 25 ms. N_D = 40 (t_2^{max} = 360 ms).

by dividing the height of the peak located at "a" (1.26 ppm) by the root-mean-square noise level between 4.3 and 4.6 ppm. The SNR would be degraded when the average evolution time (proportional to N_E and τ_{ad}) and the amplitudes of encoding and decoding gradients G_E and G_D increase, which also influence the resolution. Both the resolution and SNR should be considered when the experimental parameters are set. To gain more insight into the different effects of the pulse sequences shown in Figure 1A,B, see the experimental results on the solution of ethyl 3-bromopropionate and methanol in acetone and the solution of propanol in dimethyl sulfoxide in the Supporting Information.

A dilute solution of 97 mM ethyl 3-bromopropionate in acetone was used to further test the feasibility of our sequence for samples with low concentrations. The pulse sequence shown in Figure 1C was used to suppress the solvent peak. The

dx.doi.org/10.1021/ja1113479 |J. Am. Chem. Soc. 2011, 133, 7632–7635

parameters of the gradients in the WS module were G_1 = 6.9 G/cm, G_2 = 29.8 G/cm, δ' = 0.9 ms and G = 7.9 G/cm, δ = 2.0 ms. The same two-step phase cycling scheme was used. The length of the 90° Gauss-shaped RF pulse was 12.15 ms, corresponding to an excitation range of about 252 Hz. Considering the low SNR, the experiment was performed in a small inhomogeneous field with a line width of 110 Hz. The results are shown in Figure 3. As we can see, the spectra obtained with the same method in homogeneous and inhomogeneous fields are virtually indistinguishable (Figure 3B,B′). The average line width in the chemical shift dimension shown in Figure 3D,D′ is 32 Hz. The SNRs in Figure 3D,D′ are 62 and 48, respectively. These results indicate that our method is feasible for dilute solutions in inhomogeneous fields. Shapira et al. pointed out that the limit of detection (LOD) for a conventional single-scan 2D NMR experiment is in the range of 1−10 mM.[15] Since the single-quantum coherence signal intensity is about 10 times stronger than the iMQC signal intensity, the LOD for a two-scan iZQC experiment would be in the range of 10−100 mM.

A noteworthy advantage of our scheme is the efficiency to obtain 2D iZQC spectra. iMQCs are attractive for high-resolution NMR spectroscopy in inhomogeneous fields. However, 2D[8a,16] or 3D[17] acquisition is often required for high-resolution 1D or 2D iMQC spectra, which results in much longer experimental time than 1D experiments. The experiments would be sped up by the proposed scheme. In addition, if the solvent peak is located on one end of the spectrum, it can be removed by choosing a proper purge gradient G_P, thus reducing its influence on spectral resolution.

In summary, we incorporated an iZQC transfer scheme into the spatially encoded technique to quickly obtain high-resolution 2D *J*-resolved spectra in inhomogeneous fields. Compared to the method proposed by Pelupessy et al.,[10] the novel method can retain more straightforward spectral information such as chemical shifts and *J* multiplicity patterns. The method has the following advantages: the chemical shift information can be directly obtained from the F1 dimension, no splitting peaks are missed, and isolated spins can be detected. Moreover, our study opens a way to speed up high-resolution iMQC experiments in inhomogeneous fields. The issue of low SNR, mainly due to weaker iMQC signal intensity relative to conventional single-quantum coherence signal, is still a critical problem. NMR spectrometers with higher magnetic field, cryo probe, and dynamic nuclear polarization techniques may be used to solve it.

■ ASSOCIATED CONTENT

Supporting Information. Detailed derivation for the signals from the pulse sequence shown in Figure 1B; experimental results on the solution of ethyl 3-bromopropionate and methanol in acetone and the solution of propanol in dimethyl sulfoxide using the pulse sequences shown in Figure 1A,B. This material is available free of charge via the Internet at http://pubs.acs.org.

■ AUTHOR INFORMATION

Corresponding Author
chenz@xmu.edu.cn

■ ACKNOWLEDGMENT

This work was partially supported by the NNSF of China under Grants 10974164 and 10875101, and the Research Fund for the Doctoral Program of Higher Education of China under Grant 20090121110030.

■ REFERENCES

(1) (a) Metz, K. R.; Lam, M. M.; Webb, A. G. *Concepts Magn. Reson.* **2000**, *12*, 21–42. (b) Duh, A.; Mohoric, A.; Stepisnik, J.; Sersa, I. *J. Magn. Reson.* **2003**, *160*, 47–51.

(2) (a) Blumich, B.; Perlo, J.; Casanova, F. *Prog. Nucl. Magn. Reson. Spectrosc.* **2008**, *52*, 197–269. (b) Verpillat, F.; Ledbetter, M. P.; Xu, S.; Michalak, D. J.; Hilty, C.; Bouchard, L. S.; Antonijevic, S.; Budker, D.; Pines, A. *Proc. Natl. Acad. Sci. U.S.A.* **2008**, *105*, 2271–2273.

(3) (a) Lin, Y. Y.; Ahn, S.; Murali, N.; Brey, W.; Bowers, C. R.; Warren, W. S. *Phys. Rev. Lett.* **2000**, *85*, 3732–3735. (b) Shapira, B.; Shetty, K.; Brey, W. W.; Gan, Z. H.; Frydman, L. *Chem. Phys. Lett.* **2007**, *442*, 478–482.

(4) Hurlimann, M. D. *J. Magn. Reson.* **2007**, *184*, 114–129.

(5) (a) Meriles, C. A.; Sakellariou, D.; Heise, H.; Moule, A. J.; Pines, A. *Science* **2001**, *293*, 82–85. (b) Franck, J. M.; Demas, V.; Martin, R. W.; Bouchard, L. S.; Pines, A. *J. Chem. Phys.* **2009**, *131*, 234506.

(6) (a) Shapira, B.; Frydman, L. *J. Am. Chem. Soc.* **2004**, *126*, 7184–7185. (b) Shapira, B.; Frydman, L. *J. Magn. Reson.* **2006**, *182*, 12–21.

(7) Arthanari, H.; Frueh, D.; Wagner, G.; Pryor, B.; Khaneja, N. *J. Chem. Phys.* **2008**, *128*, 214503.

(8) (a) Vathyam, S.; Lee, S.; Warren, W. S. *Science* **1996**, *272*, 92–96. (b) Chen, Z.; Chen, Z. W.; Zhong, J. H. *J. Am. Chem. Soc.* **2004**, *126*, 446–447. (c) Huang, Y. Q.; Cai, S. H.; Lin, Y. Q.; Chen, Z. *Appl. Spectrosc.* **2010**, *64*, 235–240.

(9) Frydman, L.; Scherf, T.; Lupulescu, A. *Proc. Natl. Acad. Sci. U.S.A.* **2002**, *99*, 15858–15862.

(10) Pelupessy, P.; Rennella, E.; Bodenhausen, G. *Science* **2009**, *324*, 1693–1697.

(11) Giraudeau, P.; Akoka, S. *J. Magn. Reson.* **2007**, *186*, 352–357.

(12) Giraudeau, P.; Akoka, S. *J. Magn. Reson.* **2008**, *190*, 339–345.

(13) Liu, M. L.; Mao, X. A.; Ye, C. H.; Huang, H.; Nicholson, J. K.; Lindon, J. C. *J. Magn. Reson.* **1998**, *132*, 125–129.

(14) Chen, Z.; Hou, T.; Chen, Z. W.; Hwang, D. W.; Hwang, L. P. *Chem. Phys. Lett.* **2004**, *386*, 200–205.

(15) Shapira, B.; Lupulescu, A.; Shrot, Y.; Frydman, L. *J. Magn. Reson.* **2004**, *166*, 152–163.

(16) Chen, Z.; Cai, S. H.; Chen, Z. W.; Zhong, J. H. *J. Chem. Phys.* **2009**, *130*, 084504.

(17) Huang, Y. Q.; Chen, X.; Cai, S. H.; Cai, C. B.; Chen, Z. *J. Chem. Phys.* **2010**, *132*, 134507.